2021 23rd International Conference on Process Control (PC)
June 1–4, 2021, Štrbské Pleso, Slovakia

Control Principles of Autonomous Mobile Robots Used in Cyber-Physical Factories

Květoslav Belda
dept. of Adaptive Systems, The Czech Academy of Sciences
Institute of Information Theory and Automation
Pod Vodárenskou věží 4, 182 00 Prague 8, Czech Republic
belda@utia.cas.cz, https://orcid.org/0000-0002-1299-7704

Jan Jirsa
dept. of Technical Studies
The College of Polytechnics Jihlava
Tolstého 16, 586 01 Jihlava, Czech Republic
jan.jirsa@vspj.cz

***Abstract*—This paper introduces control principles and means applied to industrial mobile robots. These robots are a solution for batch processing of handling operations over longer distances, unlike conventional conveyor belts. They spread in cyber-physical factories in accordance with the concepts of Industry 4.0. Specific mobile robot Robotino by Festo company is considered. The principles are introduced in relation to used communication. It is realized wirelessly using WiFi and TCP/IP protocol standard. The communication is in compliance with other machines such as industrial stationary robots or technological workplaces that form basis of currently developing concept of autonomous automatic cyber-physical factories.**

***Index Terms*—mobile robot, TCP/IP communication, dynamic modeling, simulation, real-time experiments**

I. Introduction

The current industrial production is based on specific workplaces, stands which are interconnected in production lines. The manipulation operations are realized either via conveyor belts for continual synchronous production flow or by mobile units or robots used for asynchronous flow in batches and for longer distance tracks [1]. Dynamics of conveyor belts is distributed into several drives, bodies and variable loads moving on a belt and due to this characterisations, their dynamics does not lead to some generalized formulation.

However, mobile robots represent moving, generally homogenous bodies with appreciable dynamics, various problems of construction, modelling and control. They are discussed for instance in [2], [3] and [4].

This paper deals with a modeling of specific mobile robot and related control principles. Kinematic and dynamic model is introduced from robot mechanics and gears towards motors. Then, suitable representatives of non-model and model-based control principles are introduced as well as suitable software solutions such as Festo tools, MATLAB/Simulink environment including their cross connection. Using mentioned tools, the principles of modeling, control and related communication are discussed. The explanation is illustrated by time histories of simulations and real run measurements.

The work was supported by The Czech Academy of Sciences, Institute of Information Theory and Automation and The College of Polytechnics Jihlava.

II. Mobile Robot Structure

Mobile robots consist of autonomous mobile platform that is a place for a robotic arm or manipulation mechanism for picking and placing manipulated loads [5].

A mobile robot studied in this paper is the Festo Robotino®, see Fig. 1. It is an omnidirectional mobile robot equipped with three omni-wheels [6], [7], [8]. Note that in addition to omni-wheels, there are a lot of other configuration types and wheels such as castor wheels, Swedish wheels, spherical wheels etc., see [9]. The considered robot consists of platform (underframe, chassis) with three omni-directional wheels. These wheels are located at an angle of 120° to each other. Each wheel is driven autonomously by one DC motor through a planetary gearbox and a toothed belt. Here, this gearing is replaced by a single general belt gear.

Fig. 1. Mobile robot Festo Robotino®.

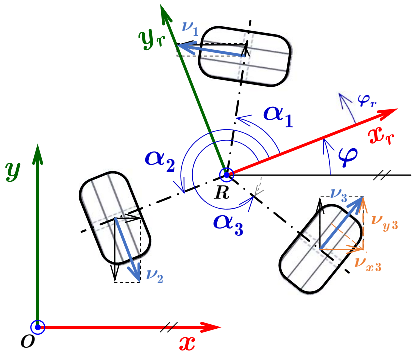

Fig. 2. Decomposition of wheel-pitch circumferential velocities.

III. Mathematical Model Analysis

In this section, detailed mathematical analysis of considered mobile robot is stated for kinematics and dynamics of the robot body and dynamics of DC drives.

A. Model of Kinematics

Since the mobile robot has no fixed Coordinate system and thus no fixed coordinates, let us define kinematic relations using velocities [9], initially between global word fixed Cartesian coordinate system and relative robot moving Cartesian coordinate system:

$$\mathcal{V} = R_\varphi^{-1}\, V \;\;\Rightarrow\;\; V = R_\varphi\, \mathcal{V} \tag{1}$$

where V and $\mathcal{V}$ are global (absolute) and relative velocity vectors, respectively:

$$\mathcal{V} = [\,\dot{x} = \nu_x,\;\; \dot{y} = \nu_y,\;\; \omega_z\,]^T \tag{2}$$

$$V = [\,\dot{x} = v_x,\;\; \dot{y} = v_y,\;\; \dot{\varphi} = \omega_z\,]^T \tag{3}$$

and R_φ is a transformation matrix of rotation around vertical axis parallel to the axis z:

$$R_\varphi = \begin{bmatrix} \cos(\varphi) & -\sin(\varphi) & 0 \\ \sin(\varphi) & \cos(\varphi) & 0 \\ 0 & 0 & 1 \end{bmatrix},\;\; R_\varphi^{-1} = R_\varphi^T \tag{4}$$

R_φ is an orthogonal matrix, therefore the indicated matrix inverse is valid. Now, let us define relation among relative velocity vector $\mathcal{V}$ and vector of circumferential velocities $\mathcal{V}_{1,2,3}$ for individual wheels.

$$\mathcal{V}_{1,2,3} = J\;\mathcal{V} \;\;\Rightarrow\;\; \mathcal{V} = J^{-1}\;\mathcal{V}_{1,2,3} \tag{5}$$

Components are defined using a principle of superposition of a general planar motion into the translation and the rotation as indicated by the following expressions:

$$\mathcal{V}_{1,2,3} = [\,\nu_1,\;\; \nu_2,\;\; \nu_3\,]^T \tag{6}$$

$$\nu_1 = -\sin\alpha_1\,\nu_{x,1} + \cos\alpha_1\,\nu_{y,1} + r\,i_w\,\omega_1 \tag{7}$$

$$\nu_2 = \sin\alpha_2\,\nu_{x,2} + \cos\alpha_2\,\nu_{y,2} + r\,i_w\,\omega_2 \tag{8}$$

$$\nu_3 = -\sin\alpha_3\,\nu_{x,3} + \cos\alpha_3\,\nu_{y,3} + r\,i_w\,\omega_3 \tag{9}$$

where angles correspond to robot drive wheel distribution: $\alpha_1 = \frac{\pi}{3} \sim 60°$, $\alpha_2 = \pi \sim 180°$ and $\alpha_3 = -\frac{\pi}{3} \sim -60° \sim \frac{5}{3}\pi \sim 300°$. When the coefficients from expressions above are separated, a Jacobian matrix J can be defined as follows

$$J = \begin{bmatrix} -\sin\alpha_1 & \cos\alpha_1 & r \\ \sin\alpha_2 & \cos\alpha_2 & r \\ -\sin\alpha_3 & \cos\alpha_3 & r \end{bmatrix} = \begin{bmatrix} -\frac{\sqrt{3}}{2} & \frac{1}{2} & r \\ 0 & -1 & r \\ \frac{\sqrt{3}}{2} & \frac{1}{2} & r \end{bmatrix} \tag{10}$$

$$J^{-1} = \begin{bmatrix} -\frac{1}{\sqrt{3}} & 0 & \frac{1}{\sqrt{3}} \\ \frac{1}{3} & -\frac{2}{3} & \frac{1}{3} \\ \frac{1}{3\,r} & \frac{1}{3\,r} & \frac{1}{3\,r} \end{bmatrix} \tag{11}$$

Then, the complete kinematic equations for velocities can be written as follows

$$\mathcal{V}_{1,2,3} = r_w\;\; i_w\;\; \Omega,\quad \Omega = [\,\omega_1,\; \omega_2,\; \omega_3\,]^T \tag{12}$$

$$V = R_\varphi\,\mathcal{V} \;=\; R_\varphi\;J^{-1}\;\mathcal{V}_{1,2,3} \tag{13}$$

$$V = \;R_\varphi\;\;J^{-1}\;\;r_w\;\;i_w\;\;\Omega \tag{14}$$

The equations above represent the total relation between vector of angular velocities of rotors of individual drive DC motors and global velocity vector V. The respective positions can be integrated according to following simple general expression:

$$s = \int_0^t v\;\mathrm{d}t,\qquad s_k = s_{k-1} + v\;T_s \tag{15}$$

where T_s is a sampling period.

B. Model of Dynamics of Robot Body

The model describing the robot dynamics can be represented by three differential equations considering, for simplicity, a one flat kinematic pair (planar joint). Let us consider two absolute positions x and y in relations to fixed origin (world coordinate system - $O\,x\,y\,z$) or relative positions x_r and y_r in relation to local robot origin (base coordinate system - $R\,x_r\,y_r\,z_r$) and relative rotation φ around vertical axis z_r.

$$m\,\ddot{x} = F_x = \sum_i F_{x,\,i},\quad i = 1,\,2,\,3 \tag{16}$$

$$m\,\ddot{y} = F_y = \sum_i F_{y,\,i} \tag{17}$$

$$I\,\ddot{\varphi} = \mathcal{T}_z = \sum_i \sqrt{F_{x,\,i}^2 + F_{y,\,i}^2}\;r = \sum_i F_i\,r \tag{18}$$

where F_x and F_y are resultant force components in corresponding directions x and y. In state-space form, the model can be written as follows

$$\dot{x} = A\,x + B\,u,\quad y = C\,x \tag{19}$$

where

$$A = \begin{bmatrix} 0_{3,3} & I_3 \\ 0_{3,3} & 0_{3,3} \end{bmatrix},\; B = \begin{bmatrix} 0_{3,3} \\ \mathrm{diag}(\frac{1}{\mathrm{m}},\frac{1}{\mathrm{m}},\frac{1}{\mathrm{I}}) \end{bmatrix},\; C = \begin{bmatrix} I_3 \\ 0_{3,3} \end{bmatrix}^T$$

and $x = [x,\, y,\, \varphi,\, \dot{x},\, \dot{y},\, \dot{\varphi}]^T$, $y = [x,\, y,\, \varphi]^T$, $u = [F_x,\, F_y,\, \mathcal{T}_z]^T$, $0_{3,3}$ and I_3 are zero and identity matrices.

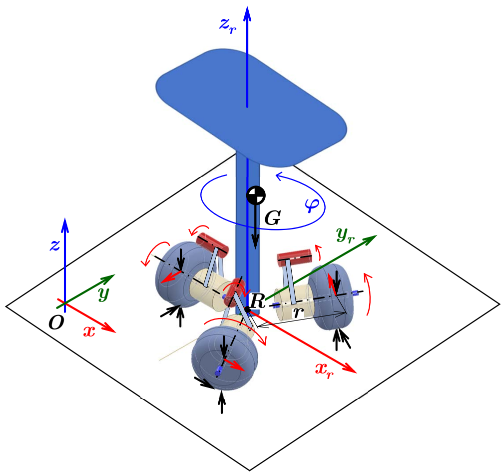

Fig. 3. Scene and distribution of force effects.

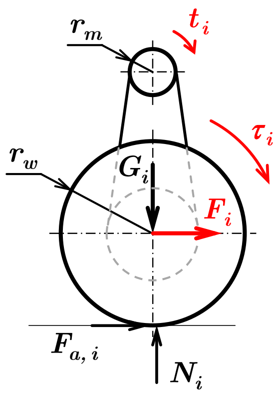

Fig. 5. Gears and force distribution in rolling motion.

The obtained generalized force effects F_x, F_y and $\mathcal{T}_z$ simplify simulation purposes. They represent releasing that corresponds to the three degrees of freedom of the substitute planar kinematic pair. The respective effects F_x, F_y and $\mathcal{T}_z$ are computed from the following system of algebraic equations:

$$
\begin{aligned}
F_{x,\,r} &= -\sin\alpha_1\, F_1 + \sin\alpha_2\, F_2 - \sin\alpha_3\, F_3 && (20)\\
F_{y,\,r} &= \cos\alpha_1\, F_1 + \cos\alpha_2\, F_2 + \cos\alpha_3\, F_3 && (21)\\
\mathcal{T}_{z,\,r} &= r\quad F_1 + \quad r\quad F_2 + \quad r\quad F_3 && (22)
\end{aligned}
$$

$$
\underbrace{\begin{bmatrix} F_{x,\,r} \\ F_{y,\,r} \\ \mathcal{T}_{z,\,r} \end{bmatrix}}_{\mathcal{F}_r} = \underbrace{\begin{bmatrix} -\sin\alpha_1 & \sin\alpha_2 & -\sin\alpha_3 \\ \cos\alpha_1 & \cos\alpha_2 & \cos\alpha_3 \\ r & r & r \end{bmatrix}}_{J^T} \begin{bmatrix} F_1 \\ F_2 \\ F_3 \end{bmatrix} \qquad (23)
$$

Note that $\alpha_1 = \frac{\pi}{3}$, $\alpha_2 = \pi$ and $\alpha_3 = -\frac{\pi}{3} \sim \frac{5}{3}\pi$. Respective driving forces F_1, F_2 and F_3 are computed from the following system of algebraic equations $\mathcal{F} = [F_x,\ F_y,\ \mathcal{T}_z]^T$:

$$
\begin{bmatrix} F_1 \\ F_2 \\ F_3 \end{bmatrix} = (J^T)^{-1}\, R_\varphi^T \begin{bmatrix} F_x \\ F_y \\ \mathcal{T}_z \end{bmatrix}, \quad \mathcal{F}_r = R_\varphi^T\, \mathcal{F} \qquad (24)
$$

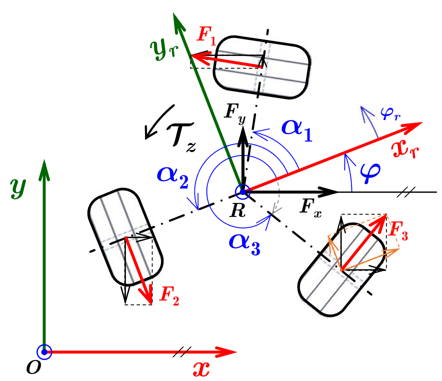

Fig. 4. Resultant force effects.

$$
R_\varphi^T = \begin{bmatrix} \cos(\varphi) & \sin(\varphi) & 0 \\ -\sin(\varphi) & \cos(\varphi) & 0 \\ 0 & 0 & 1 \end{bmatrix},\ (J^T)^{-1} = \begin{bmatrix} -\frac{1}{\sqrt{3}} & \frac{1}{3} & \frac{1}{3\,r} \\ 0 & -\frac{2}{3} & \frac{1}{3\,r} \\ \frac{1}{\sqrt{3}} & \frac{1}{3} & \frac{1}{3\,r} \end{bmatrix} \quad (25)
$$

F_x, F_y and $\mathcal{T}_z$ are resultant force effects based on three driving forces F_1, F_2 and F_3. These forces are excited by transmitted torques τ_1, τ_2 and τ_3 from source torques t_1, t_2 and t_3 of appropriate electric motors described in Sec. III-D:

$$
F_1 = \frac{\tau_1}{r_w},\quad F_2 = \frac{\tau_2}{r_w},\quad F_3 = \frac{\tau_3}{r_w} \qquad (26)
$$

$$
t_i = \tau_i\, i_w,\quad i_w = \frac{r_m}{r_w},\quad i = 1,\,2,\,3 \qquad (27)
$$

C. Condition of Rolling Motion

In order to keep the real rolling motion of robot wheels as a superposition of two motions – translations with respect to the surface (floor) and rotation around their own axes, three respective conditions are necessary to be considered:

$$
N_i\,\mu \le F_i \le F_{a,i} = N_i\,\mu_a,\quad i = 1,\,2,\,3 \qquad (28)
$$

where μ is a running resistance and μ_a is a coefficient of adhesion friction, $F_{a,i}$ are adhesion forces and N_i is a normal vector (normal reaction) defined as:

$$
N_i = -\,G_i,\quad i = 1,\,2,\,3 \qquad (29)
$$

Individual components G_1, G_2 and G_3 of gravitation effect G acting in centre of gravity can be determined using the following system of algebraic equations:

$$
\begin{aligned}
x:\ & G_1\, x_{r,\,1} + G_2\, x_{r,\,2} + G_3\, x_{r,\,3} = G\, x_{r,\,T} && (30)\\
y:\ & G_1\, y_{r,\,1} + G_2\, y_{r,\,2} + G_3\, y_{r,\,3} = G\, y_{r,\,T} && (31)\\
\texttt{f}:\ & G_1 + G_2 + G_3 = G && (32)\\
& G = m\, g && (33)
\end{aligned}
$$

where m is a total robot mass and g is gravitational constant. It is given by an asymmetric force distribution, see Fig. 6.

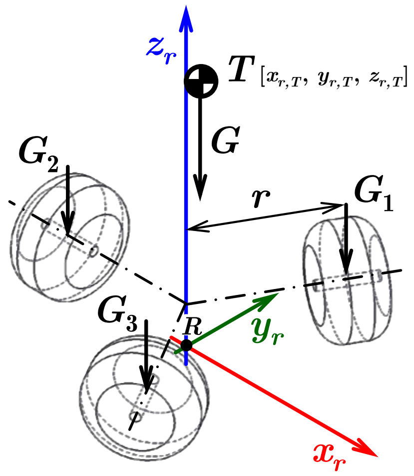

Fig. 6. Decomposition of gravitational effects into individual wheels.

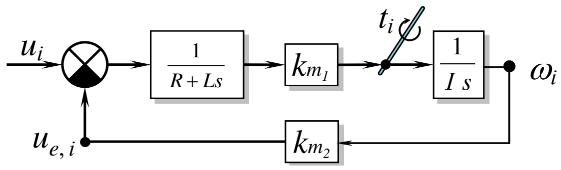

Fig. 7. Diagram of the DC motor.

The appropriate matrix form is:

$$\begin{bmatrix} x_{r,1} & x_{r,2} & x_{r,3} \\ y_{r,1} & y_{r,2} & y_{r,3} \\ 1 & 1 & 1 \end{bmatrix} \begin{bmatrix} G_1 \\ G_2 \\ G_3 \end{bmatrix} = \begin{bmatrix} G\,x_{r,T} \\ G\,y_{r,T} \\ G \end{bmatrix} \tag{34}$$

where $x_{r,i} = r\,\cos\alpha_i$ and $y_{r,i} = r\,\sin\alpha_i$, $\alpha_1 = \frac{\pi}{3}$, $\alpha_2 = \pi$, $\alpha_3 = \frac{5\,\pi}{3} \sim -\frac{\pi}{3}$. Then, the result is:

$$\begin{bmatrix} G_1 \\ G_2 \\ G_3 \end{bmatrix} = \begin{bmatrix} \frac{1}{3\,r} & \frac{1}{\sqrt{3}\,r} & \frac{1}{3} \\ -\frac{2}{3\,r} & 0 & \frac{1}{3} \\ \frac{1}{3\,r} & -\frac{1}{\sqrt{3}\,r} & \frac{1}{3} \end{bmatrix} \begin{bmatrix} G\,x_{r,T} \\ G\,y_{r,T} \\ G \end{bmatrix} \tag{35}$$

D. Model of Dynamics of Drives

The DC motor represents the simplest motor configuration. It can be modelled by the second order equation as follows:

$$\ddot{t}_i + \frac{R}{L}\,\dot{t}_i + \frac{k_{m1}\,k_{m2}}{I\,L}\,t_i = \frac{k_{m1}}{L}\,\dot{u}_i \tag{36}$$

The diagram in Fig. 7 shows the brush DC motor with permanent magnet in the stator, where u, u_e are input and internal induced voltages; t_i are torques that correspond to the expression (27) of their transformation into torques on individual wheels; I is moment of inertia of the motor shaft and other parameters R, L, k_{m1}, k_{m2} are electrical constants: resistance, inductance, current and voltage constants.

It is possible to consider a simplification of the mathematical model by the following expression:

$$u_i = \frac{R}{k_{m1}}\,t_i \tag{37}$$

It follows from the assumption of the steady state behavior of the particular unit. Then, the model of motor dynamics can be given for small powers by the indicated linear function [1].

IV. Control Principles

This section briefly shows representatives of non-model and model-based control approaches suitable for application to autonomous mobile robots. Note that successfulness and accuracy of the robot motion depends not only on control algorithm but also on the quality of the robot odometry system.

A. PID/PSD Controllers

Continuous PID and discrete PSD controllers are representatives of non-model-based control approaches. Usual form, considered for Robotino control is the following

$$u(t) = K_p \left(e(t) + \frac{1}{T_i} \int_0^t e(t)\,\mathrm{d}t + T_d\,\dot{e}(t) \right) \tag{38}$$

and its discrete incremental form is:

$$\begin{aligned} u_k = u_{k-1} + K_p \Bigg(& (e_k - e_{k-1}) \\ & + \frac{1}{T_i}\,e_k\,T_s + T_d\,\frac{e_k - 2\,e_{k-1} + e_{k-2}}{T_s} \Bigg) \end{aligned} \tag{39}$$

B. Model Predictive Control

The discrete model predictive control is the representative of model-based control with optimality criterion [10]:

$$\begin{aligned} & \min_{\Delta U_k} J_k\,(\hat{Y}_{k+1},\, W_{k+1},\, \Delta U_k) \\ & \text{subject to state-space model (19)} \\ & \text{and constraints:} \quad \begin{array}{ccccc} y_{min} & \le & y_{j+1} & \le & y_{max} \\ u_{min} & \le & u_j & \le & u_{max} \end{array} \end{aligned} \tag{40}$$

where $\hat{Y}_{k+1}$, W_{k+1} and ΔU_k are vectors of output predictions, reference values and increments of searched control actions $u_k = u_{k-1} + \Delta u_k$, respectively; $j = k, \cdots, k+N$ and N is a prediction horizon. The cost behaviour is expressed by quadratic function as follows:

$$J_k = ||Q_{YW}\,(\hat{Y}_{k+1} - W_{k+1})||_2^2 + ||Q_{\Delta U}\,\Delta U_k||_2^2 \tag{41}$$

Due to multi-step prediction horizon N, predictive control is very beneficial for the robot motion in unknown environment with some sequential scene detection.

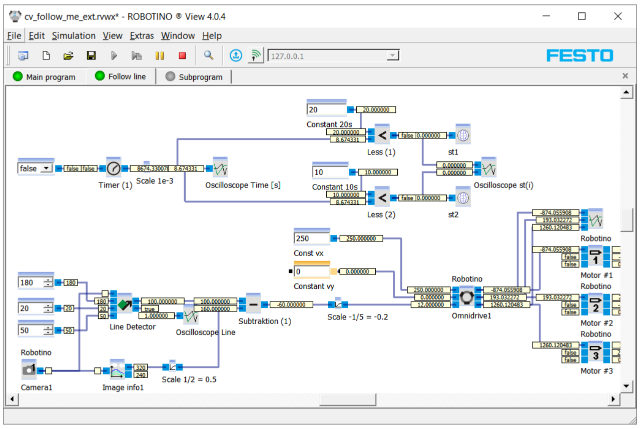

Fig. 8. Robotino View.

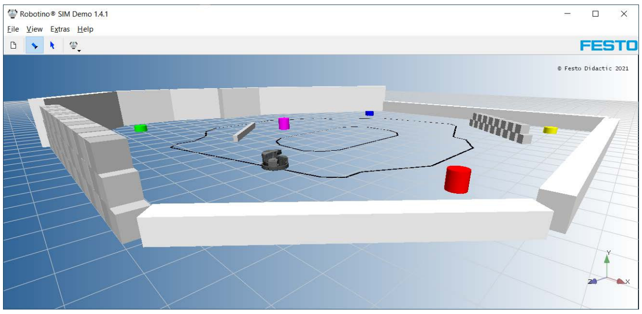

Fig. 9. Robotino SIM Demo.

V. Implementation Using Festo Software

This section introduces example of control implementation using Festo tool “Robotino View” as a programming environment and “Robotino SIM Demo” as a simulation and visualisation tool [7] - see figures Fig. 8 and Fig. 9. These tools serve for comparative tests. The both belong to freeware solutions as distinct from MATLAB/Simulink environment.

VI. Implementation Using MATLAB/Simulink

Fig. 10 shows modeling with Simulink/Simscape lib that can visualize 3D model by Mechanics explorer - Fig. 11.

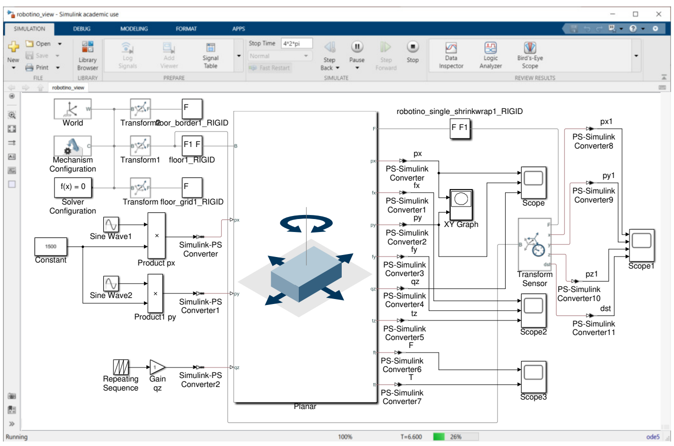

Fig. 10. Simulink/Simscape model of the robot motion.

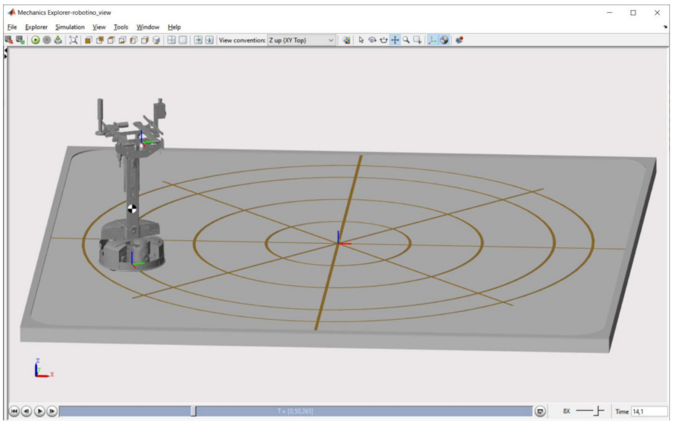

Fig. 11. Mechanics explorer with the Robotino mobile robot.

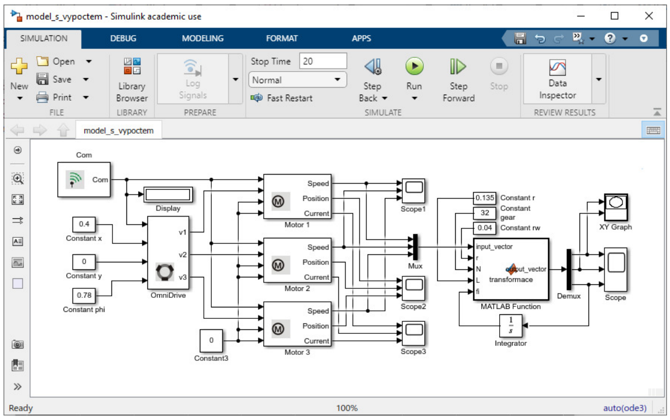

Fig. 12. Simulink model with Festo toolbox.

Another way is the Festo toolbox for MATLAB/Simulink that has the similar programming structure as the original Festo “Robotino View” tool - Fig. 12. This toolbox contains comparable set of blocks. In comparison with freeware “Robotino View” [7], it offers standard user-friendly MATLAB/Simulink environment.

VII. Simulation and Experimental Examples

This section briefly demonstrates tests with the models and the real robot. Fig. 13 and Fig. 14 show simulation using Simulink and Simscape library, where physical parameters as position of the center of gravity, masses and geometrical dimensions were given by 3D CAD model that corresponds to the real mobile robot Robotino®.

Fig. 15 and Fig. 16 show one representative record of real experiments with the real robot Robotino® using Festo Toolbox for MATLAB/Simulink. In the robot motion, it is visible a deviation caused by uncertain influences of the robot environment such as an uneven floor or wheel slips. It is caused by free robot movement without any fixed reference coordinate system. The realized control works on level of increments. It integrates increments of position without periodic calibration to some fixed reference system. Then, the robot drifts from desired reference values.

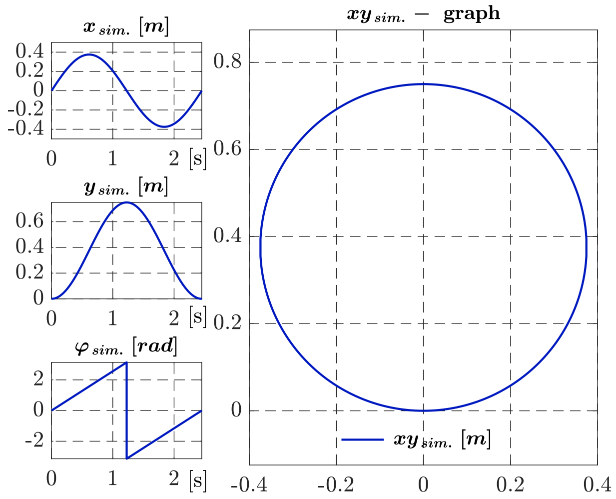

Fig. 13. Time histories of absolute Cartesian coordinates x, y and φ.

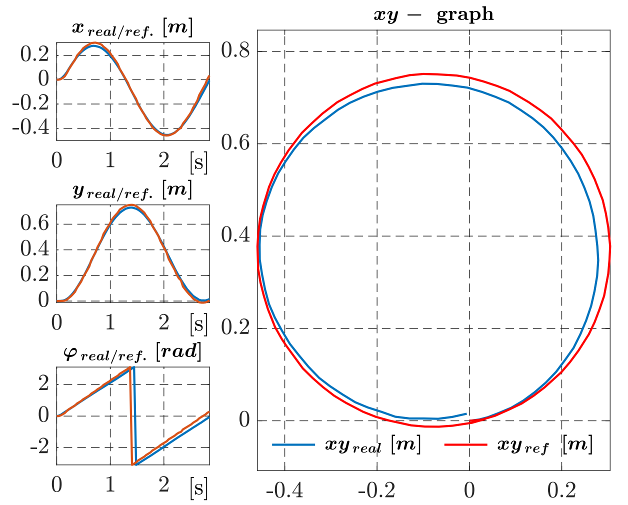

Fig. 15. Time histories of absolute Cartesian coordinates x, y and φ.

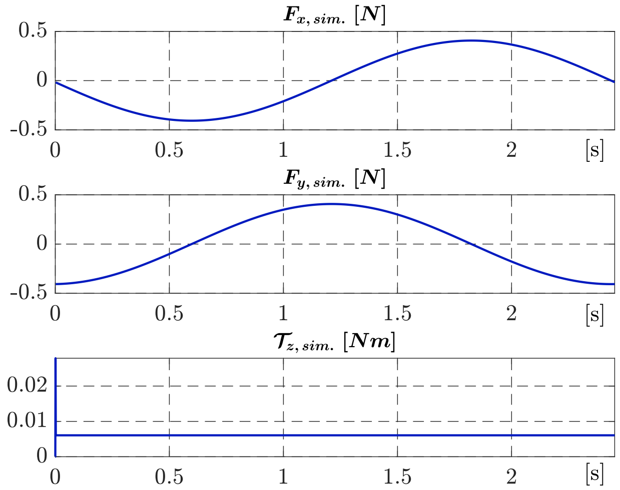

Fig. 14. Time histories of generalized force effects F_x, F_y and $\mathcal{T}_z$.

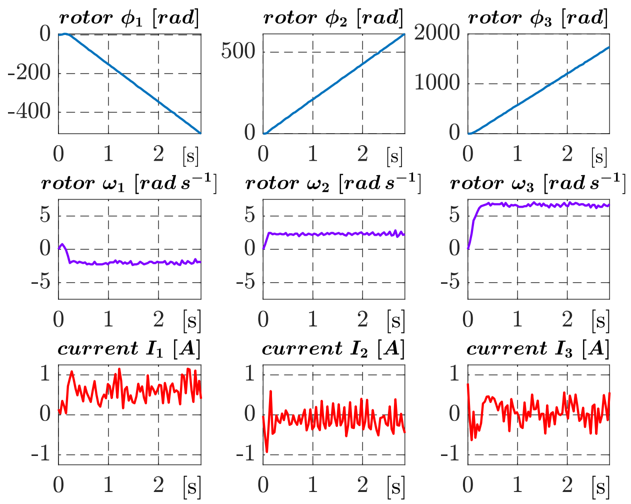

Fig. 16. Time histories of motor positions ϕ_i, speeds ω_i and currents I_i.

Let us, for instance, consider different situation when fixed reference is available. Such a reference can be realized by a specific fixed path marked e.g. by strips on the floor, see black strips in Fig. 9. Then, the robot is able to follow such strips and to suppress undesirable error of increments due to existence of fixed strip reference.

VIII. Conclusion

The paper introduces control principles including detailed mathematical physical analysis. The mathematical models, both kinematic and dynamic, were applied in simulation (both models) and in real experiment (kinematic model). There is a demonstration of various software tools that are available not only for simulations but also for experiments. It was demonstrated by time histories of physical quantities.

References

[1] K. Belda and P. Píša, "Design and modelling of distributed industrial manipulation system with wireless operated moving manipulation," *Trans. on Electrical Engineering*, vol. 4, no. 3, pp. 69–75, 2015.

[2] V. Damić, M. Čohodar, and A. Omerspahić, "Dynamic analysis of an omni-directional mobile robot," *J. Trends in the Develop. of Machinery and Assoc. Tech.*, vol. 17, no. 1, pp. 153–156, 2013.

[3] L. Raj and A. Czmerk, "Modelling and simul. of the drivetrain of an omnidirect. mob. robot," *Automatika*, vol. 58, no. 2, pp. 232–243, 2017.

[4] C. Caceres, J. Rosário, and D. Amaya, "Design, simulation, and control of an omnidirectional mobile robot," *J. Int. Review of Mechanical Engineering (IREME)*, vol. 12, no. 4, pp. 382–389, 2018.

[5] K. Belda and O. Rovný, "Predictive control of 5 dof robot arm of autonomous mobile robotic syst. motion control employing math. model of the robot arm dynamics," in *Proc. 21th Int. Conf. Process Control*, Štrbské Pleso, SK, 2017, pp. 339–344.

[6] Festo, "Robotino," [access 22-November-2020]. [Online]. Available: https://ip.festo-didactic.com/InfoPortal/Robotino/Overview/EN/index.html

[7] Robotino Wiki, "Robotino Wiki," [access 22-November-2020]. [Online]. Available: https://wiki.openrobotino.org/

[8] K. Sharma, F. Dušek, and D. Honc, "Comparative study of predictive controllers for traj. tracking of non-holonomic mobile robot," in *Proc. 21th Int. Conf. Process Control*, Štrbské Pleso, SK, 2017, pp. 197–203.

[9] R. Siegwart and I. Nourbakhsh, *Introduction to Autonomous Mobile Robots*. London, GB: MIT Press, 2004.

[10] K. Belda, "On-line solution os system constraints in generalized predictive control design," in *Proc. of the 20th Int. Conf. on Process Control*, Štrbské Pleso, SK, 2015, pp. 25–30.